# The cutoff method for the numerical computation of nonnegative solutions of parabolic PDEs with application to anisotropic diffusion and lubrication-type equations

Changna Lu* Weizhang Huang† Erik S. Van Vleck‡

The cutoff method, which cuts off the values of a function less than a given number, is studied for the numerical computation of nonnegative solutions of parabolic partial differential equations. A convergence analysis is given for a broad class of finite difference methods combined with cutoff for linear parabolic equations. Two applications are investigated, linear anisotropic diffusion problems satisfying the setting of the convergence analysis and nonlinear lubrication-type equations for which it is unclear if the convergence analysis applies. The numerical results are shown to be consistent with the theory and in good agreement with existing results in the literature. The convergence analysis and applications demonstrate that the cutoff method is an effective tool for use in the computation of nonnegative solutions. Cutoff can also be used with other discretization methods such as collocation, finite volume, finite element, and spectral methods and for the computation of positive solutions.

**AMS 2010 Mathematics Subject Classification.** 65M06, 35K51
**Key Words.** cutoff, projection, nonnegative solution, positive solution, error analysis, finite difference, anisotropic diffusion, lubrication-type equation
**Abbreviated title.** Cutoff method for computation of nonnegative solutions

## 1 Introduction

Many physical phenomena involve variables such as the density and concentration of a material that take only nonnegative values. The mathematical reflection of this property is that the partial differential equations (PDEs) modeling the phenomena admit nonnegative solutions. For the numerical

*College of Math and Statistics, Nanjing University of Information Science and Technology, Nanjing, Jiangsu 210044, China. (luchangna@nuist.edu.cn)
†Department of Mathematics, the University of Kansas, Lawrence, KS 66045, U.S.A. (huang@math.ku.edu)
‡Department of Mathematics, the University of Kansas, Lawrence, KS 66045, U.S.A. (evanvleck@math.ku.edu)

solution of those PDEs, it is crucial that numerical schemes preserve the solution nonnegativity and produce physically meaningful numerical solutions.

A closely related concept is the maximum principle. Preserving the maximum principle is equivalent to preserving the solution nonnegativity for linear problems [50] but generally the former is more difficult than the latter. It is known (e.g., see [11]) that a conventional numerical method, such as a finite difference (FD), finite volume (FV), or finite element (FE) method, generally does not preserve the maximum principle and can produce negative undershoot in the solution for diffusion problems, especially those with heterogeneous anisotropic diffusion coefficients. Considerable effort has been made on developing numerical schemes satisfying the maximum principle; e.g., see [6, 7, 10, 11, 28, 29, 31, 34, 46, 47, 51, 52] for steady-state isotropic diffusion problems and [15, 22, 23, 27, 30, 36, 38, 39, 40, 41, 42, 45] for steady-state anisotropic diffusion problems. Particularly, Ciarlet and Raviart [11] show that the linear FE approximation of an elliptic isotropic diffusion problem satisfies the maximum principle when the mesh is simplicial and nonobtuse. The result is generalized to anisotropic diffusion problems by Huang and his coworkers in [27, 36, 41]. On the other hand, less progress has been made for time dependent problems. For example, Fujii [21] shows that the linear FE approximation of the heat equation satisfies the maximum principle when the mesh is simplicial and acute and the time step size is bounded above by a bound proportional to the squared maximal element size and below by a bound proportional to the squared minimal element in-diameter. He also shows that when the lumped mass matrix is used, the maximum principle holds without requiring the time step size to be bounded from below. Fujii's results are extended to more general isotropic diffusion problems by Faragó et al. [17, 19, 20] and to anisotropic diffusion problems by Li and Huang [37]. Faragó and Horváth [18] study the relations between the maximum principle, nonnegativity preservation, and maximum norm contractivity for linear parabolic equations and their finite difference and Galerkin finite element discretizations. Thomée and Wahlbin [50] consider more general parabolic PDEs and show that the maximum principle cannot hold for the conventional semidiscrete FE problem and Fujii's conditions on the mesh are essentially sharp for the lumped mass matrix. Le Potier [32, 33] (also see Lipnikov et al. [39]) proposes two nonlinear FV schemes for linear anisotropic diffusion problems and shows that they are second order in space and satisfy monotonicity [32] or the maximum principle [33].

We consider initial-boundary value problems of parabolic PDEs which are well posed and have a unique, nonnegative solution. Instead of employing a maximum-principle preserving scheme, we propose to use the cutoff method that cuts off the negative values in the computed solution at each time step and then continues the time integration with the corrected solution; see Fig. 1 for a sketch of the solution procedure. The cutoff method shares a similar idea with many projection and correction methods. For example, projection methods [9, 49] are an effective means of enforcing the incompressibility condition in the numerical solution of time dependent incompressible fluid flow problems. Projection is also used by some researchers in the numerical solution of Hamiltonian systems to preserve the energy; e.g., see [26]. A FE/implicit Euler discretization of a Cahn-Hilliard equation with logarithmic nonlinearity is considered in [13] and iterative methods to solve the resulting nonlinear systems of equations are developed to keep the solution within its physically relevant range. Solution compression is used in the design of maximum-principle-satisfying high order schemes for scalar conservation laws by Zhang and Shu [53]. It should be emphasized that the cutoff method provides several advantages over many positivity-preserving or maximum-principle-preserving schemes. Its implementation is simple and requires no significant changes in the existing code. Moreover, the cutoff procedure does not impose any constraint on the mesh and time step which maximum-principle-preserving schemes often impose. However, unlike projection methods, there do not seem to exist published theoretical or numerical studies on the cutoff method.

The objective of this paper is to provide a theoretical and numerical study of the cutoff method for use in the computation of nonnegative solutions of parabolic PDEs. We shall first prove that a broad class of finite difference methods are convergent when they are incorporated with the cutoff method for linear parabolic PDEs. Two applications are then investigated. The first is a linear anisotropic diffusion problems which satisfies the setting of the convergence analysis. It is known that a conventional finite difference or finite element method with a uniform or quasi-uniform mesh does not preserve the maximum principle (nor the solution nonnegativity) and typically produces negative undershoot in the computed solution. The cutoff method removes the unphysical negative values in the solution while keeping the same convergence order of the underlying scheme. The second application is nonlinear lubrication-type equations. It is unclear if the convergence analysis (which can be extended to some nonlinear equations; see Remark 2.1) applies to those equations. A distinct feature of lubrication-type equations is that a positive solution can develop a finite time singularity of the form $u \to 0$ and become identically zero on some spatial interval for a period of time. A conventional finite difference or finite element method can produce negative values in the computed solution during this development of singularity. Negative solution values are not only unphysical but also cease the computation for typical situations where the nonlinear diffusion coefficients are undefined for negative solution values. The application of the cutoff method avoids this difficulty. Moreover, it is shown that no regularization is needed when cutoff is used. Numerical results are shown to be in good agreement with existing ones in the literature.

The outline of the paper is as follows. The cutoff method is described and some of its properties are given in Section 2. The convergence of a broad class of finite difference methods is proved also in Section 2 when they are incorporated with the cutoff method for the computation of nonnegative solutions of linear parabolic PDEs. Application of finite difference methods with cutoff to a linear anisotropic diffusion problem and a lubrication-type PDE is studied in Sections 3 and 4, respectively. Finally, Section 5 contains conclusions and further comments.

## 2 The cutoff method and convergence analysis

In this section, we first describe the cutoff method and some of its properties. We then give a convergence analysis of the method for a class of finite difference methods applied to linear parabolic problems. Possible generalizations are also discussed.

### 2.1 The cutoff method

Consider a continuous function $f = f(\boldsymbol{x})$ defined on a domain $\Omega \subset \mathbb{R}^d$ ($d \geq 1$). For any given cutoff parameter $\delta \in \mathbb{R}$, we define the $\delta$-cutoff function as

$$f_\delta^+(\boldsymbol{x}) = \begin{cases} f(\boldsymbol{x}), & \text{for } f(\boldsymbol{x}) \geq \delta \\ \delta, & \text{for } f(\boldsymbol{x}) \leq \delta \end{cases} \quad \forall \boldsymbol{x} \in \Omega. \tag{1}$$

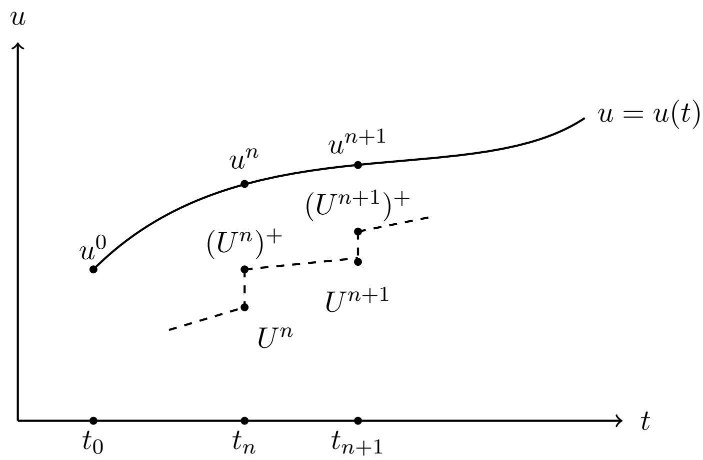


Figure 1: An illustration of the time integration with cutoff (the dashed line). Here, $U^n$ is the numerical solution, $(U^n)^+$ is the corrected numerical solution and $u(t)$ is the exact solution of the IBVP starting from $u^0$ at $t = t_0$.

Note that $f^+(\boldsymbol{x}) \equiv f_0^+(\boldsymbol{x})$ is the nonnegative part of $f$, i.e.,

$$f^+(\boldsymbol{x}) = \frac{1}{2}(|f(\boldsymbol{x})| + f(\boldsymbol{x})) = \begin{cases} f(\boldsymbol{x}), & \text{for } f(\boldsymbol{x}) \geq 0 \\ 0, & \text{for } f(\boldsymbol{x}) \leq 0 \end{cases} \quad \forall \boldsymbol{x} \in \Omega. \tag{2}$$

The following three lemmas give some properties of cutoff functions. Although these properties are easy to prove (and almost obvious), they play a central role in the convergence analysis for a class of finite difference methods in the next subsection.

**Lemma 2.1.** *For a given function $f$ and any nonnegative continuous function $u$ defined on $\Omega$, we have*

$$|f^+(\boldsymbol{x}) - u(\boldsymbol{x})| \leq |f(\boldsymbol{x}) - u(\boldsymbol{x})|, \quad \forall \boldsymbol{x} \in \Omega. \tag{3}$$

**Proof.** Obviously, (3) holds when $f(\boldsymbol{x}) \geq 0$. When $f(\boldsymbol{x}) < 0$, we have $f^+(\boldsymbol{x}) = 0$. By assumption, $u(\boldsymbol{x}) \geq 0$. Thus, we have

$$|f^+(\boldsymbol{x}) - u(\boldsymbol{x})| = |u(\boldsymbol{x})| \leq |f(\boldsymbol{x})| + |u(\boldsymbol{x})| = |f(\boldsymbol{x}) - u(\boldsymbol{x})|.$$

□

**Lemma 2.2.** *For a given function $f$ and any nonnegative continuous function $u$ defined on $\Omega$, we have*

$$|f^+(\boldsymbol{x}) - f(\boldsymbol{x})| \leq |u(\boldsymbol{x}) - f(\boldsymbol{x})|, \quad \forall \boldsymbol{x} \in \Omega. \tag{4}$$

**Proof.** The proof is similar to that of Lemma 2.1. □

**Lemma 2.3.** *Given a cutoff parameter $\delta \geq 0$, for any function $f$ and any nonnegative continuous function $u$ defined on $\Omega$, we have*

$$|f_\delta^+(\boldsymbol{x}) - f^+(\boldsymbol{x})| \leq \delta, \quad \forall \boldsymbol{x} \in \Omega \tag{5}$$

$$|f_\delta^+(\boldsymbol{x}) - u(\boldsymbol{x})| \leq |f(\boldsymbol{x}) - u(\boldsymbol{x})| + \delta, \quad \forall \boldsymbol{x} \in \Omega. \tag{6}$$

**Proof.** Inequality (5) follows from the definitions of $f^+$ and $f_\delta^+$. Inequality (6) follows from the triangle inequality $|f_\delta^+(\boldsymbol{x}) - u(\boldsymbol{x})| \le |f^+(\boldsymbol{x}) - u(\boldsymbol{x})| + |f_\delta^+(\boldsymbol{x}) - f^+(\boldsymbol{x})|$ and Lemma 2.1. $\square$

## 2.2 Error analysis for a linear IBVP problem

We now use the results in the previous subsection to analyze the convergence of a class of finite difference schemes for a general initial-boundary value problem (IBVP) in the form

$$\begin{cases} \frac{\partial u}{\partial t} = L(u), \quad \text{in} \quad \Omega \times (t_0, T] \\ u = g, \quad \text{on} \quad \partial\Omega \\ u = u^0, \quad \text{on} \quad \Omega \times \{t = t_0\} \end{cases} \tag{7}$$

where $\Omega \subset \mathbb{R}^d$ $(d \ge 1)$ is the physical domain, $L$ is a linear elliptic differential operator and $g$ and $u^0$ are given sufficiently smooth functions. We assume that the IBVP is well posed and admits a unique nonnegative continuous solution, $u = u(t, \boldsymbol{x})$. We also assume that $L$ and $g$ do not contain $t$ explicitly for notational simplicity.

We consider a class of finite difference schemes for (7) in the matrix form as

$$B_1 U^{n+1} = B_0 U^n + F^n, \tag{8}$$

where $B_0$ and $B_1$ are matrices independent of $n$ and $U^n$ is an approximation of the exact solution at $t = t_n$, i.e., $U^n = \{U_j^n\}$, $u^n = \{u_j^n\}$, $U_j^n \approx u_j^n \equiv u(t_n, \boldsymbol{x}_j)$ for each mesh vertex $\boldsymbol{x}_j$. We assume that (8) satisfies

$$\|B_1^{-1}\| \le K_1, \tag{9}$$

$$\|B_1^{-1} B_0\| \le (1 + K\Delta t), \tag{10}$$

$$\frac{1}{\Delta t}\left[B_1 u^{n+1} - B_0 u^n - F^n\right] \longrightarrow \frac{\partial u}{\partial t} - L(u), \quad \text{as} \quad \Delta t(h) \to 0 \tag{11}$$

where $\Delta t$ and $h$ are the maximal time step size and the maximal element size, respectively, $K$ and $K_1$ are positive constants, and $\|\cdot\|$ is a proper matrix norm. Condition (9) requires that (8) produce a bounded solution while (10) and (11) are the stability and consistency conditions, respectively. The local truncation error of this scheme is defined as

$$\tau^n = B_1 u^{n+1} - B_0 u^n - F^n. \tag{12}$$

Assume that scheme (8) is $(p, q)$-order for some positive integers $p$ and $q$. Then, there exists a constant $C_{lte}(u)$ (depending only on the exact solution) such that

$$\|\tau^n\| \le C_{lte}(u)\, \Delta t\, (\Delta t^p + h^q). \tag{13}$$

It is remarked that there exist many schemes satisfying assumptions (9) – (11). Examples include those employing central finite differences for spatial discretization and the $\theta$-method for temporal discretization; e.g., see Morton and Mayers [43].

**Theorem 2.1.** *Assume that IBVP (7) is well posed and admits a unique nonnegative continuous exact solution $u = u(t, \boldsymbol{x})$. We also assume that scheme (8) satisfies (9) – (11) and (13). Then, the error for the cutoff solution procedure shown in Fig. 1 with scheme (8) is bounded by*

$$\|(U^n)^+ - u^n\| \le \|U^n - u^n\| \le \frac{K_1}{K}\, e^{Kt_n}\, C_{lte}(u)\, (\Delta t^p + h^q). \tag{14}$$

**Proof.** Let $e^n = U^n - u^n$. Notice that the cutoff solution procedure shown in Fig. 1 with (8) satisfies

$$B_1 U^{n+1} = B_0 (U^n)^+ + F^n. \tag{15}$$

Combining this with (12), we obtain

$$B_1 e^{n+1} = B_0((U^n)^+ - u^n) - \tau^n.$$

It follows that

$$\|e^{n+1}\| \le \|B_1^{-1} B_0\| \cdot \|(U^n)^+ - u^n\| + \|B_1^{-1}\| \cdot \|\tau^n\|.$$

Combining this with (9) and (10) leads to

$$\|e^{n+1}\| \le (1 + K\Delta t)\, \|(U^n)^+ - u^n\| + K_1\, \|\tau^n\|. \tag{16}$$

Lemma 2.1 implies

$$\|(U^n)^+ - u^n\| \le \|U^n - u^n\|. \tag{17}$$

Thus, we get

$$\|e^{n+1}\| \le (1 + K\Delta t)\, \|e^n\| + K_1\, \|\tau^n\|. \tag{18}$$

Then it is standard to show that (14) follows from (13) and (18). □

**Remark 2.1.** From the above proof we can see that the key condition is the convergence of the original scheme (without cutoff). If it (without cutoff) is convergent, using Lemma 2.1 we can readily show that the scheme with cutoff is also convergent. This observation implies that the convergence analysis of the cutoff method can be extended to more general linear or nonlinear IBVPs. □

When a strictly positive solution is desired, we can replace $(U^n)^+$ with $(U^n)^+_\delta$ for some positive constant $\delta$. The following theorem can be proven using Lemma 2.3 in a similar way as for Theorem 2.1.

**Theorem 2.2.** *Assume that IBVP (7) is well posed and admits a unique nonnegative continuous exact solution $u = u(t, \boldsymbol{x})$. We also assume that scheme (8) satisfies (9) – (11) and and (13). For the cutoff solution procedure shown in Fig. 1 with scheme (8) and with $(U^n)^+$ being replaced with $(U^n)^+_\delta$ for some positive $\delta$, the error is bounded by*

$$\|(U^n)^+_\delta - u^n\| \le \frac{K_1}{K}\, e^{Kt_n}\, C_{lte}(u)\, (\Delta t^p + h^q) + \left( \frac{(1 + K\Delta t)}{K\Delta t}\, e^{Kt_n} + 1 \right) \delta. \tag{19}$$

**Remark 2.2.** Inequality (19) shows that $\delta$ should be chosen proportional to $\Delta t$ for the error bound to stay bounded as $\Delta t \to 0$. Ideally, $\delta$ should be at the same level as the local truncation error, i.e.,

$$\delta = \mathcal{O}(\Delta t(\Delta t^p + h^q)). \tag{20}$$

This way, the terms on the right-hand side of (19) have the same convergence order as $\Delta t(h) \to 0$. □

## 3 An anisotropic diffusion problem

In this section we present numerical results obtained for a 2D linear anisotropic diffusion problem by the cutoff method described in the previous section. The problem takes the form of IBVP (7) with

$$L(u) = \nabla \cdot (\mathbb{D}\, \nabla u) + f, \quad \Omega = [0,1] \times [0,1], \quad \mathbb{D} = \begin{pmatrix} 500.5 & 480 \\ 480 & 500.5 \end{pmatrix}, \tag{21}$$

and $f$, $u^0$, and $g$ are chosen such that the exact solution of the IBVP is given by

$$u = \frac{1}{2}\exp(-t)(\tanh(-15(x-y)) + 1). \tag{22}$$

The problem satisfies the maximum principle and the solution stays between 0 and 1.

It is worth pointing out that unlike lubrication-type equations which we shall consider in the next section, for this problem the computation can continue when negative values occur in the computed solution. From this point of view, it is unnecessary to remove negative values at each time step. Nevertheless, this problem satisfies the setting of the convergence analysis in the previous section and provides a good example for verifying the theory and testing the effectiveness and accuracy of the cutoff method.

We use Cartesian grids of size $J \times J$ for the physical domain, central finite differences for spatial discretization, and a third-order singly diagonally implicit Runge-Kutta (SDIRK) method [1, 8] for temporal discretization of the underlying PDE. The discretization is standard and can be shown to be convergent with order $(3, 2)$ (third order in time and second order in space). It is also known (and is shown below) that this standard scheme does not preserve the maximum principle and produces spurious undershoot and overshoot in the numerical solution. The numerical results presented below are obtained with a fixed time step size $\Delta t = 10^{-2}$, which was found to be small enough so that the temporal discretization error is ignorable compared to the spatial discretization error.

Fig. 2 shows the surface plot of a numerical solution (after cutoff) at $t = 1$. The contours of the numerical solutions before and after cutoff are shown in Fig. 3 (a) and (b). One may notice that the underlying finite difference scheme does not preserve the nonnegativity and the numerical solution at $t = 1$ contains negative values (with $U^N_{min} = -1.073 \times 10^{-3}$ where $N$ is the last time step) before cutoff.

The $L^2$ error, $\|(U^N)^+ - u^N\|_{L^2(\Omega)}$, and the maximal undershoot, $-u_{min}$, are shown in Fig. 4 as functions of the number of subintervals in $x$ (or $y$) direction. We can see that the $L^2$ error decreases at a rate of $O(J^{-2})$ (second order in terms of element size) as $J$ increases. This is consistent with the theoretical prediction given in Theorem 2.1. On the other hand, the maximal undershoot, which is equal to the cutoff error, i.e., $-u_{min} = \|U^N - (U^N)^+\|_\infty$, decreases at a faster rate. This is somewhat surprising since we expect the cutoff error to be at the level of the local truncation error, which is second order in space.

Recall that the cutoff strategy can be used to preserve the positivity of the solution. For example, when the cutoff parameter is taken $\delta = \Delta t(\Delta x)^2$, we have $(U^n_j)^+_\delta \geq \Delta t(\Delta x)^2$. Theorem 2.2 implies that the $L^2$ error, $\|(U^N)^+_\delta - u^N\|_{L^2(\Omega)}$, decreases at a rate of second order in space. For the current example, the numerical results obtained with this cutoff parameter are indistinguishable from those shown in Figs. 3 and 4. For this reason and to save space, we omit those results here.

It is worth mentioning that computations were also performed for a similar problem with a convection term,

$$L(u) = \nabla \cdot (\mathbb{D}\, \nabla u) - \boldsymbol{b} \cdot \nabla u + f, \tag{23}$$

where $\mathbb{D}$ is given in (21), $\boldsymbol{b} = [1000, 1000]^T$, and the functions $f$, $g$, and $u^0$ are chosen such that the exact solution is given by (22). The obtained results (not shown) are very similar to those shown in Figs. 3 and 4.

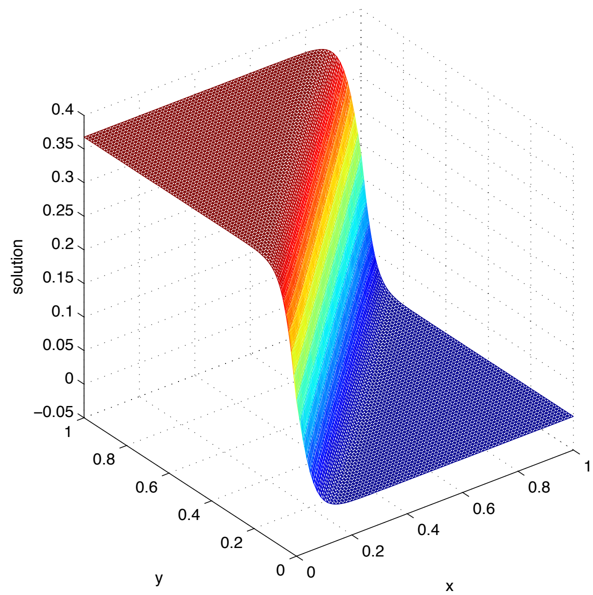


Figure 2: Example (21). The surface plot of a numerical solution (after cutoff) at $t = 1$ obtained with an $80 \times 80$ Cartesian grid.

## 4 Application to lubrication-type equations

In this section we consider the application of the cutoff method to a lubrication-type equation, which was first derived from lubrication theory by Greenspan [24] for describing the movement of thin viscous films and spreading droplets. Lubrication theory consists of a depth-averaged equation of mass conservation and a simplified form of the Navier-Stokes equations that is appropriate for a thin layer of very viscous fluid. We consider a lubrication-type equation in the general form

$$u_t + \nabla \cdot (f(u)\nabla \Delta u) = 0, \quad f(u) \sim u^n, \;\; n \in [0, \infty) \tag{24}$$

where $u$ is the thickness of the viscous droplet and $n$ is a physical parameter which has different values for different boundary conditions on the liquid solid interface. Lubrication-type equations also appear in several other applications, including a thin neck model in the Hele-Shaw cell [12], Cahn-Hilliard models with degenerate mobility [16], and problems in population dynamics [35] and plasticity [25].

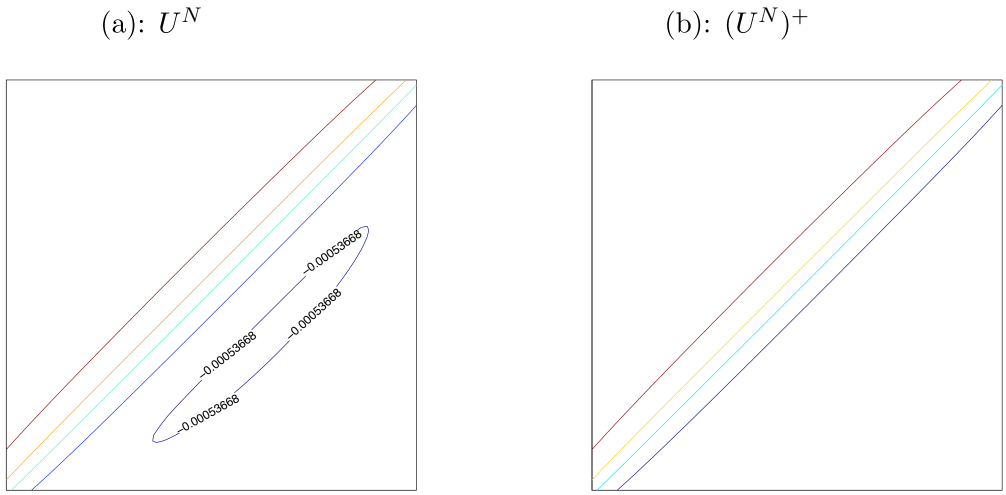


Figure 3: Example (21). Contours of the numerical solutions at $t = 1$ before and after cutoff. The solutions are obtained with an $80 \times 80$ Cartesian grid.

It is noted that the solution $u$ must stay nonnegative to be physically meaningful in all of those applications.

It is known theoretically [2, 5] that in one dimension, (24) preserves the positivity of the solution for $n \geq 3.5$ and has a nonnegative weak solution in a sense of distributions for $3/8 < n < 3$ (and in a weaker sense for $0 < n < 3/8$). Such a weak solution can be obtained [2] as the limit as $\epsilon \to 0$ of the solution of the regularized problem

$$u_t^\epsilon + \nabla \cdot (f^\epsilon(u^\epsilon)\nabla\Delta u^\epsilon) = 0, \quad f^\epsilon(u^\epsilon) = \frac{(u^\epsilon)^4 f(u^\epsilon)}{\epsilon f(u^\epsilon) + (u^\epsilon)^4}, \tag{25}$$

where $\epsilon > 0$ is the regularization parameter. Moreover, numerical computation (such as see [3, 4, 5]) shows that for small values of $n > 0$, a positive solution can first develop a finite time singularity of the form $u \to 0$ at some point (which physically describes the rupture of the liquid film), then becomes identically zero on an interval of time dependent length for a period of time, becomes positive again at a later time, and eventually decays to the mean of the initial solution. It is challenging to simulate this singularity development since conventional numerical methods do not preserve the nonnegativity of the solution and requires a huge number of mesh points to provide the necessary resolution to avoid spurious, negative undershoot. Moreover, when $n$ is an even denominator rational number, $f(u)$ is undefined for negative $u$. In this situation, the computation typically stops around the initial formation of the singularity when negative values start to appear in the numerical solution. For this reason, the simulation of the singularity development in (24) is a good test for the cutoff method although it is unclear if the convergence analysis described in § 2.2 applies to (24).

Great effort has been made in the numerical solution of (24). In addition to the above mentioned references [3, 4, 5], Zhornitskaya and Bertozzi [54] propose a positivity preserving finite difference scheme for the regularized equation (25). Russell et al. [44] solve the same regularized equation using a moving collocation method. Sun et al. [48] solve (24) in two dimensions using an adaptive finite

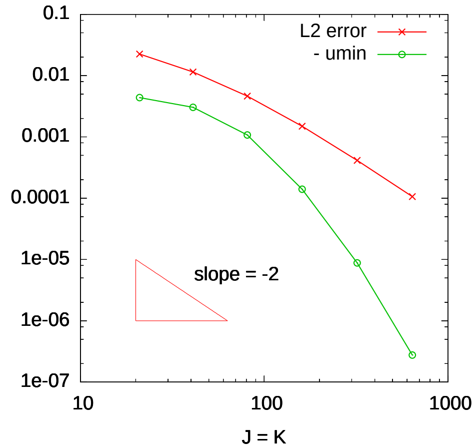


Figure 4: Example (21). The $L^2$ error, $\|(U^N)^+ - u^N\|_{L^2(\Omega)}$, and the maximal undershoot, $-u_{min}$, are shown as functions of the number of subintervals in $x$ (or $y$) direction.

element method and show that proper mesh adaptation can provide accurate resolution and there is no need to use regularization in the numerical simulation of the singularity development in (24).

We first consider an IBVP of the one-dimensional lubrication-type equation as

$$\begin{cases} u_t + (f(u)u_{xxx})_x = 0, \quad x \in \Omega \equiv (-1,1), \quad f(u) = u^{\frac{1}{2}}, \\ u(t, \pm 1) = 0, \; u_{xxx}(t, \pm 1) = 0, \\ u(0,x) = 0.8 - \cos(\pi x) + 0.25\cos(2\pi x). \end{cases} \tag{26}$$

Notice that the initial condition is strictly positive (with minimum value 0.05 and mean value 0.8) and $f(u)$ is undefined for negative $u$. We use a uniform mesh of $J$ cells for $\Omega$, central finite differences for spatial discretization, a third-order SDIRK method for the temporal discretization of the underlying PDE. (A small fixed time step $\Delta t = 10^{-6}$ is used in our computation.) This discretization is basically the same as that for the example in the previous section except that a special treatment is needed for the diffusion coefficient for the current problem since it is nonlinear. Recall that the scheme does not preserve the nonnegativity of the solution. Thus, iterates can have negative values at some point during the Newton iterative solution of the nonlinear algebraic equations resulting from the SDIRK/finite difference discretization of the underlying PDE. Once this occurs, the computation stops because $f(u)$ is undefined for those values. One way to avoid this difficulty is to use $f((U^{n+1})^+)$ instead of $f(U^{n+1})$ in the scheme. However, the nonsmoothness of $(U^{n+1})^+$ can cause difficulty in the convergence of the Newton iteration. We use here the "lagged diffusivity" method, i.e., the diffusion coefficient is computed using the (corrected) numerical solution at the previous time step. An iterative method based on the lagged diffusivity is used and proved to be convergent by Dobson and Vogel [14] for a total variation denoising problem which also has a nonlinear diffusion coefficient.

Fig. 5 shows a numerical solution at various time instants obtained with the cutoff method (without using regularization for $f(u)$) on a relatively coarse uniform mesh of 129 points. The result is almost identical (in the eyeball norm) to those in [3, 48]. To further verify the result, the computation is done with a uniform mesh of 1001 points and the obtained solution is indistinguishable from the one shown in Fig. 5 in the plotting precision.

A uniform mesh of 1001 points is used for the numerical study of the singularity development of the solution. Fig. 6 shows the close views of the solution during the development. It can be seen that the singularity is developed at around $t = 7.30 \times 10^{-4}$, which is consistent with existing numerical simulations, including those in [54] with a positivity-preserving scheme. Then, the solution becomes identically zero on an interval of time dependent length for a period of time. The length of the interval increases from zero, attains its maximum (about 0.12), and decreases to zero. Afterward, the solution becomes positive again, and eventually decays to the mean of the initial solution. It is known (e.g., see [3]) that the development of the singularity is characterized by the third order derivative of the solution becoming infinite at certain points. This can be seen in Fig. 7 where the third order derivative of the numerical solution is shown at various time instants. In particular, the third order derivative becomes discontinuous when the singularity occurs, then has jump discontinuities, and then becomes continuous again when the solution is positive.

As we have seen in the above, there is no need to use any regularization for $f(u)$ (cf. (25)) with the cutoff method. On the other hand, it is interesting to see the effects of the regularization of $f(u)$ on the solution. We first point out that the regularization does not guarantee the nonnegativity of the solution for the central finite difference discretization on a uniform mesh. Thus, we also need to use the cutoff method for the regularized equation (25). A solution obtained for (25) (with $\epsilon = 10^{-14}$) with the cutoff method is shown in Fig. 8. By a direct comparison with Fig. 7, one can see that there is only a slight difference (at the level of $\mathcal{O}(10^{-6})$) in the onset time and disappearance time of the singularity. Moreover, the solution of the regularized problem does not become identically zero on an interval for a period of time. Instead, there is a bump at the central part of the interval and the height of the bump maintains constant almost for the whole appearance period of singularity. Once again, the length of the interval first increases from zero, reaches its maximum, and decreases to zero when the solution becomes positive again.

Fig. 9 shows comparison of numerical solutions at onset of singularity and at $t = 0.001$. It can be seen that the regularization changes the onset pattern: the solution to the non-regularized equation touches the $x$-axis at one point whereas those to the regularized one touch at two points simultaneously. Moreover, the length of the touching interval and the height of the bump at onset depend on the regularization parameter $\epsilon$. The smaller $\epsilon$, the smaller the touching interval and the lower the bump. This suggests $u^\epsilon \to u$ as $\epsilon \to 0$. It is interesting to point out that all solutions, for regularization or non-regularization, have almost the same length of the touching interval at $t = 0.001$.

Finally, we present some numerical results for an IBVP of the two-dimensional lubrication-type equation as

$$\begin{cases} u_t + \nabla \cdot (f(u) \nabla \Delta u) = 0, \quad (x,y) \in \Omega \equiv [-1,1] \times [-1,1], \quad f(u) = u^{\frac{1}{2}}, \\ u = 0, \;\; \frac{\partial \Delta u}{\partial n} = 0, \quad (x,y) \in \partial\Omega \\ u(0,x,y) = (0.8 - \cos(\pi x) + 0.25\cos(2\pi x))(0.8 - \cos(\pi y) + 0.25\cos(2\pi y)), \quad (x,y) \in \Omega. \end{cases} \tag{27}$$

Fig. 10 (a) shows a numerical solution at $t = 0.001$ obtained with a uniform mesh of size $81 \times 81$ while its profiles along the diagonal line $x = y$ at various times are shown in Fig. 10 (b). One can see that the development of singularity has a similar behavior as in one dimension (cf. Fig. 5). One may also see that the onset time for the current example is slightly earlier. This is because the current initial solution has a smaller minimum value 0.025. The contours of the numerical solutions at $t = 0.001$

before and after cutoff are shown in Fig. 11. The undershoot (with $u_{min} = -3.23 \times 10^{-4}$) is visible in the solution before cutoff. These results demonstrate that the cutoff method can be used for the simulation of singularity development in the two-dimensional lubrication-type problem without need of any type of regularization.

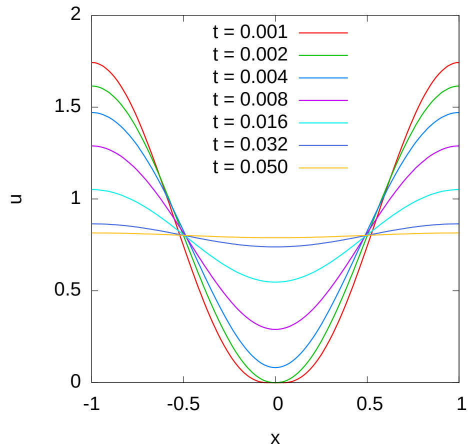


Figure 5: The one-dimensional lubrication-type problem. The solution obtained with 129 uniform grid points is shown at various time instants.

## 5 Conclusions and further comments

In the previous section we have studied the cutoff method for the numerical computation of nonnegative solutions of parabolic partial differential equations. Several properties of the cutoff method are given in Lemmas 2.1 – 2.3. Convergence of a class of finite difference methods is proved (Theorems 2.1 and 2.2) when they are incorporated with the cutoff method for linear parabolic PDEs. The method is investigated for two applications, linear anisotropic diffusion problems and nonlinear lubrication-type PDEs. The numerical results are consistent with theoretical predictions and in good agreement with existing results in the literature.

We have considered finite difference methods in this work. But it is worth pointing out that the cutoff method can also be used with other discretization methods, e.g. collocation, finite volume, finite element, or spectral methods. As an example, we show in Figs. 12 and 13 results obtained with the standard linear finite element method on Delaunay meshes for anisotropic diffusion problem (21). They are comparable with those in Figs. 3 and 4. Theoretical analysis for finite element methods with the cutoff strategy is currently underway.

**Acknowledgment.** The work was supported in part by the National Science Foundation (U.S.A.) under Grants DMS-1115118 and DMS-1115408 and the Natural Science Foundation of China under Grant 40906048.

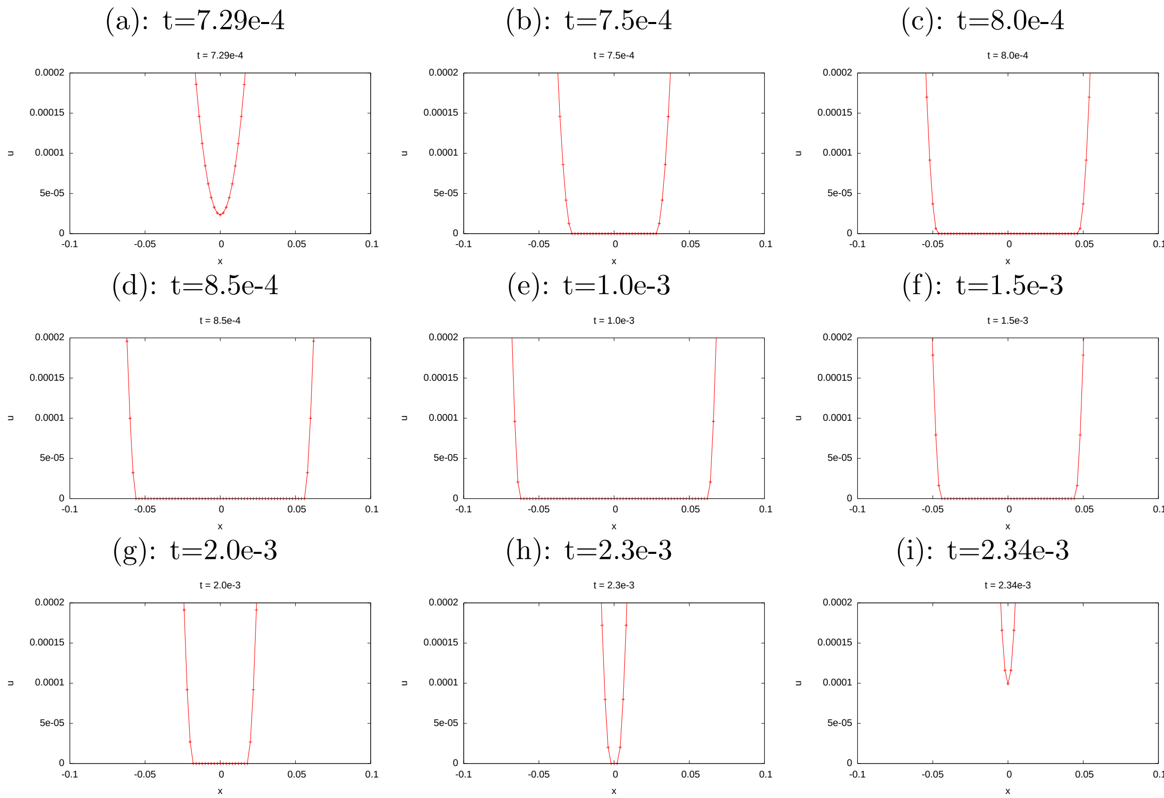


Figure 6: The one-dimensional lubrication-type problem. The close views of the numerical solution are shown at various time instants during the singularity development. The numerical solution is obtained by the cutoff method (without using regularization for $f(u)$) on a uniform mesh of 1001 points with $\Delta t = 10^{-6}$.

## References


[1] R. Alexander. Diagonally implicit Runge-Kutta methods for stiff O.D.E.'s. *SIAM J. Numer. Anal.*, 14:1006 – 1021, 1977.

[2] F. Bernis and A. Friedman. Higher order nonlinear degenerate parabolic equations. *J. Differential Equations*, 83:179–206, 1990.

[3] A. L. Bertozzi. Loss and gain of regularity in a lubrication equation for thin viscous films. In *Free boundary problems: theory and applications (Toledo, 1993)*, volume 323 of *Pitman Res. Notes Math. Ser.*, pages 72–85. Longman Sci. Tech., Harlow, 1995.

[4] A. L. Bertozzi. Symmetric singularity formation in lubrication-type equations for interface motion. *SIAM J. Appl. Math.*, 56:681–714, 1996.

[5] A. L. Bertozzi, M. P. Brenner, T. F. Dupont, and L. P. Kadanoff. Singularities and similarities in interface flows. In *Trends and perspectives in applied mathematics*, volume 100 of *Appl. Math. Sci.*, pages 155–208. Springer, New York, 1994.

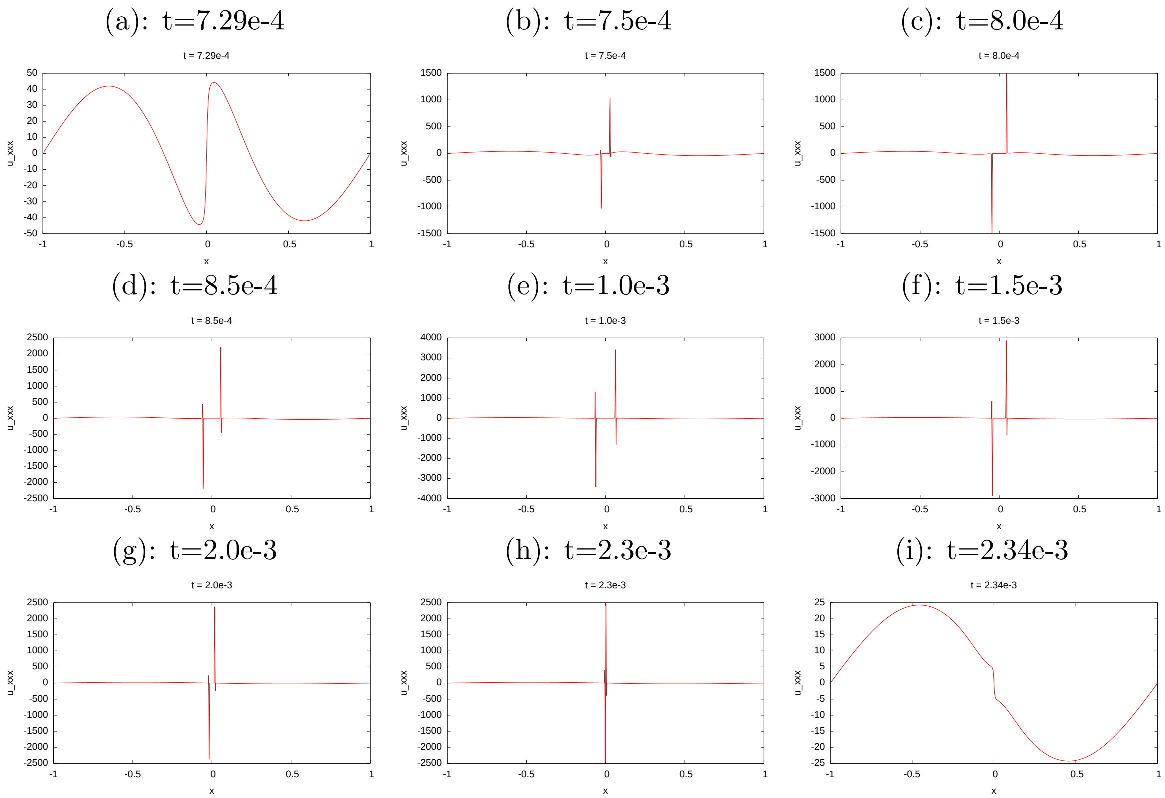


Figure 7: The one-dimensional lubrication-type problem. The close views of the third order derivative of the numerical solution are shown at various time instants during the singularity development. The numerical solution is obtained by the cutoff method (without using regularization for $f(u)$) on a uniform mesh of 1001 points with $\Delta t = 10^{-6}$.

[6] J. Brandts, S. Korotov, and M. Křížek. The discrete maximum principle for linear simplicial finite element approximations of a reaction-diffusion problem. *Lin. Alg. Appl.*, 429:2344–2357, 2008.

[7] E. Burman and A. Ern. Discrete maximum principle for Galerkin approximations of the Laplace operator on arbitrary meshes. *C. R. Acad. Sci. Paris*, Ser.I 338:641–646, 2004.

[8] J. R. Cash. Diagonally implicit runge-kutta formulae with error estimates. *J. Inst. Math. Appl.*, 24:293–301, 1979.

[9] A. J. Chorin. Numerical solution of the navier-stokes equations. *Math. Comp.*, 22:745 – 762, 1968.

[10] P. G. Ciarlet. Discrete maximum principle for finite difference operators. *Aequationes Math.*, 4:338–352, 1970.

[11] P. G. Ciarlet and P.-A. Raviart. Maximum principle and uniform convergence for thefinite element method. *Comput. Meth. Appl. Mech. Engrg.*, 2:17–31, 1973.

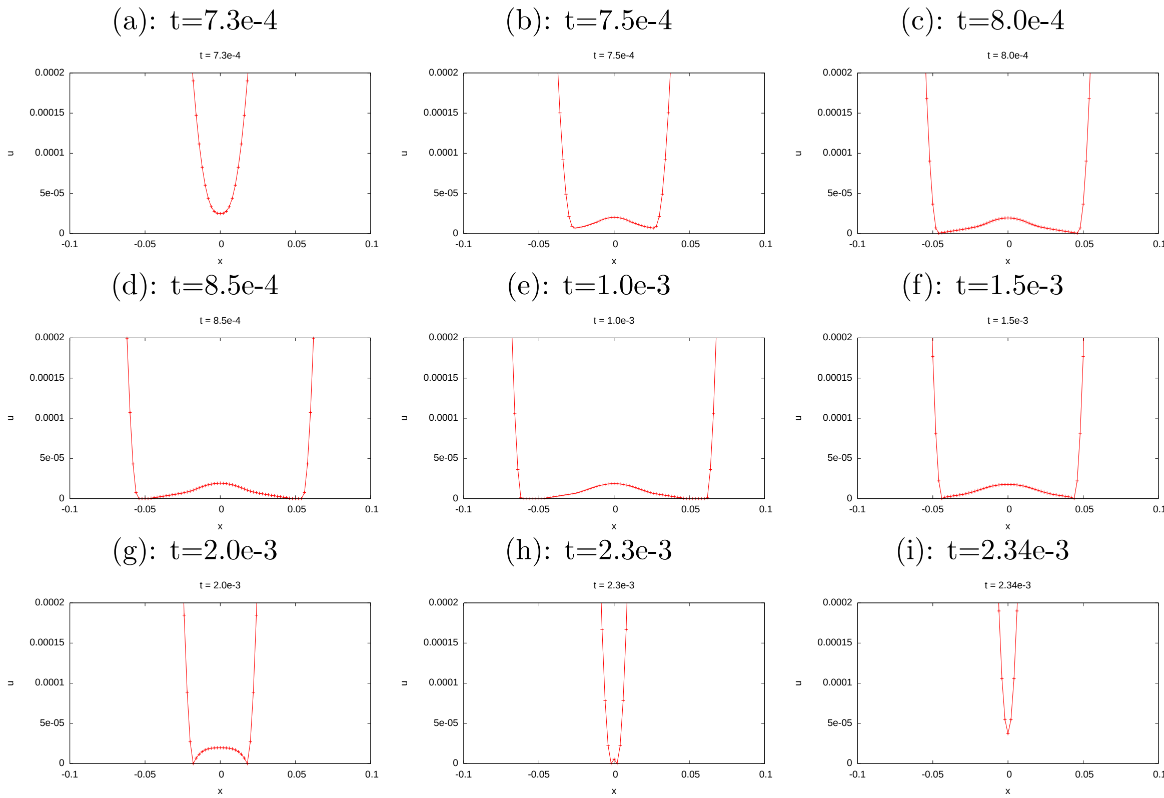


Figure 8: The one-dimensional regularized lubrication-type problem (with $\epsilon = 10^{-14}$). The close views of the numerical solution are shown at various time instants during the singularity development. The numerical solution is obtained by the cutoff method with regularization for $f(u)$ on a uniform mesh of 1001 points with $\Delta t = 10^{-6}$.


[12] P. Constantin, T. F. Dupont, R. E. Goldstein, L. P. Kadanoff, M. J. Shelley, and S.-M. Zhou. Droplet breakup in a model of the Hele-Shaw cell. *Phys. Rev. E (3)*, 47:4169–4181, 1993.

[13] M. I. M. Copetti and C. M. Elliott. Numerical analysis of the Cahn-Hilliard equation with a logarithmic free energy. *Numer. Math.*, 63:39–65, 1992.

[14] D. C. Dobson and C. R. Vogel. Convergence of an iterative method for total variation denoising. *SIAM J. Numer. Anal.*, 34:1779–1791, 1997.

[15] A. Drăgănescu, T. F. Dupont, and L. R. Scott. Failure of the discrete maximum principle for an elliptic finite element problem. *Math. Comp.*, 74:1–23, 2004.

[16] C. M. Elliott and H. Garcke. On the Cahn-Hilliard equation with degenerate mobility. *SIAM J. Math. Anal.*, 27:404–423, 1996.

[17] I. Faragó and R. Horváth. On the nonnegativity conservation of finite element solutions of parabolic problems. In *Finite element methods (Jyväskylä, 2000)*, volume 15 of *GAKUTO Internat. Ser. Math. Sci. Appl.*, pages 76–84. Gakkōtosho, Tokyo, 2001.

(a): Solutions at onset of singularity (b): Solutions at $t = 0.001$

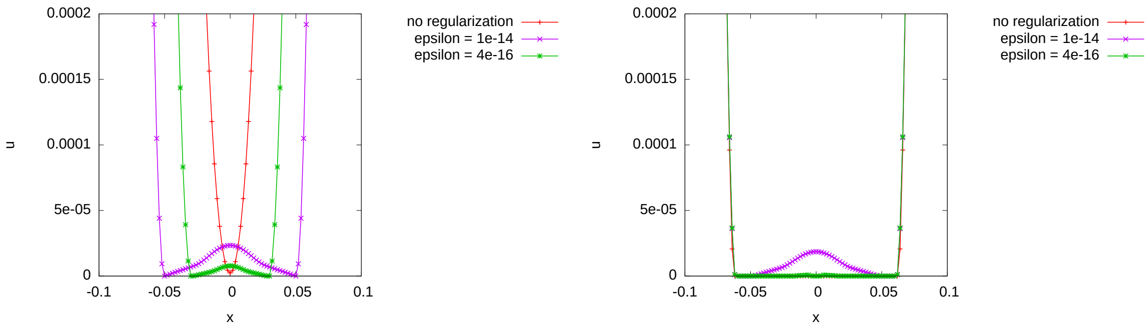


Figure 9: The one-dimensional lubrication-type problem with/without regularization. Numerical solutions at onset of singularity or at $t = 0.001$.

(a): Numerical solution at $t = 0.001$ (b): Solution along $x = y$ at various times

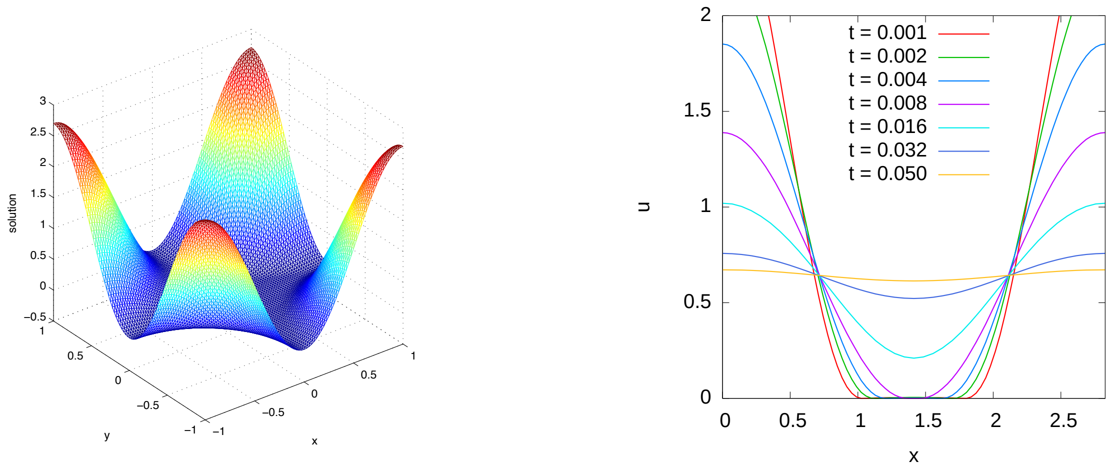


Figure 10: The two-dimensional lubrication problem. The solution is obtained with the cutoff method with a uniform mesh of size $81 \times 81$.


[18] I. Faragó and R. Horváth. Discrete maximum principle and adequate discretizations of linear parabolic problems. *SIAM J. Sci. Comput.*, 28:2313–2336, 2006.

[19] I. Faragó, R. Horváth, and S. Korotov. Discrete maximum principle for linear parabolic problems solved on hybrid meshes. *Appl. Numer. Math.*, 53:249–264, 2005.

[20] I. Faragó, R. Horváth, and S. Korotov. Discrete maximum principles for FE solutions of nonstationary diffusion-reaction problems with mixed boundary conditions. *Numer. Methods Partial Differential Equations*, 27:702–720, 2011.

[21] H. Fujii. Some remarks on finite element analysis of time-dependent field problems. In *Theory and Proactice in Finite Element Structural Analysis*, pages 91–106. University of Tokyo, Tokyo, 1973.

(a): $U^N$ (b): $(U^N)^+$

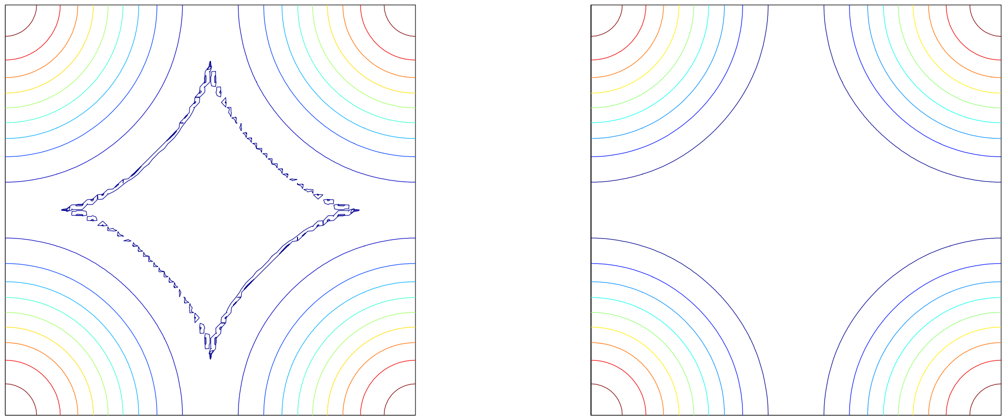

Figure 11: The two-dimensional lubrication problem. Contours of the numerical solutions at $t = 0.001$ before and after cutoff.


[22] S. Gűnter and K. Lackner. A mixed implicit-explicit finite difference scheme for heat transport in magnetised plasmas. *J. Comput. Phys.*, 228:282–293, 2009.

[23] S. Gűnter, Q. Yu, J. Kruger, and K. Lackner. Modelling of heat transport in magnetised plasmas using non-aligned coordinates. *J. Comput. Phys.*, 209:354–370, 2005.

[24] H. P. Greenspan. On the motion of a small viscous droplet that wets a surface. *J. Fluid Mech.*, 84:125–143, 1978.

[25] G. Grün. Degenerate parabolic differential equations of fourth order and a plasticity model with non-local hardening. *Z. Anal. Anwendungen*, 14:541–574, 1995.

[26] E. Hairer. Long-time energy conservation of numerical integrators. In *Foundations of computational mathematics, Santander 2005*, volume 331 of *London Math. Soc. Lecture Note Ser.*, pages 162–180. Cambridge Univ. Press, Cambridge, 2006.

[27] W. Huang. Discrete maximum principle and a delaunay-type mesh condition for linear finite element approximations of two-dimensional anisotropic diffusion problems. *Numer. Math. Theory Meth. Appl.*, 4:319–334, 2011. (arXiv:1008.0562).

[28] J. Karátson and S. Korotov. An algebraic discrete maximum principle in Hilbert space with applications to nonlinear cooperative elliptic systems. *SIAM J. Numer. Anal.*, 47:2518–2549, 2009.

[29] J. Karátson, S. Korotov, and M. Křížek. On discrete maximum principles for nonlinear elliptic problems. *Math. Comput. Sim.*, 76:99–108, 2007.

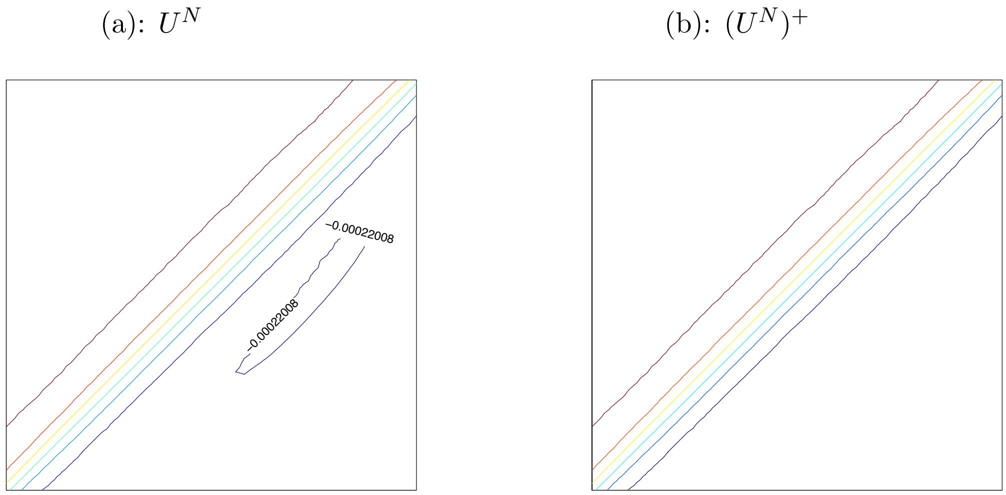


Figure 12: The standard linear finite element method for Example (21). Contours of the numerical solutions at $t = 1$ before and after cutoff obtained with a Delaunay mesh of $N = 2350$ elements.

[30] D. Kuzmin, M. J. Shashkov, and D. Svyatskiy. A constrained finite element method satisfying the discrete maximum principle for anisotropic diffusion problems. *J. Comput. Phys.*, 228:3448–3463, 2009.

[31] M. Křížek and Q. Lin. On diagonal dominance of stiffness matrices in 3D. *East-West J. Numer. Math.*, 3:59–69, 1995.

[32] C. Le Potier. Schéma volumes finis monotone pour des opérateurs de diffusion fortement anisotropes sur des maillages de triangles non structurés. *C. R. Math. Acad. Sci. Paris*, 341:787–792, 2005.

[33] C. Le Potier. Un schéma linéaire vérifiant le principe du maximum pour des opérateurs de diffusion très anisotropes sur des maillages déformés. *C. R. Math. Acad. Sci. Paris*, 347:105–110, 2009.

[34] F. W. Letniowski. Three-dimensional Delaunay triangulations for finite element approximations to a second-order diffusion operator. *SIAM J. Sci. Stat. Comput.*, 13:765–770, 1992.

[35] M. A. Lewis. Spatial coupling of plant and herbivore dynamics: The contribution of herbivore dispersal to transient and persistent "waves" of damage. *Theoret. Population Biol.*, 45:277–312, 1994.

[36] X. P. Li and W. Huang. An anisotropic mesh adaptation method for the finite element solution of heterogeneous anisotropic diffusion problems. *J. Comput. Phys.*, 229:8072–8094, 2010 (arXiv:1003.4530v2).

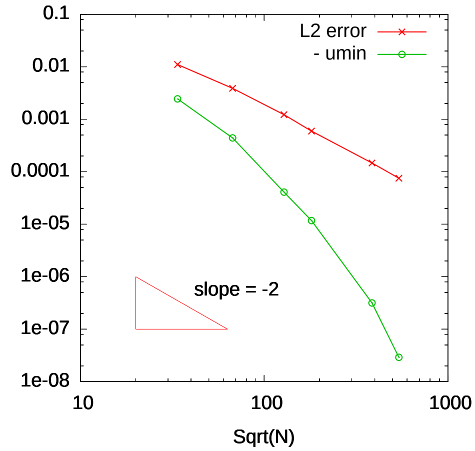


Figure 13: The standard linear finite element method for Example (21). The $L^2$ error, $\|(U^N)^+ - u^N\|_{L^2(\Omega)}$, and the maximal undershoot, $-u_{min}$, are shown as functions of $\sqrt{N}$ with $N$ being the number of elements.


[37] X. P. Li and W. Huang. Maximum principle for the finite element solution of time dependent anisotropic diffusion problems. *Numer. Meth. P.D.E.*, 2012. (arXiv:1209.5657).

[38] X. P. Li, D. Svyatskiy, and M. Shashkov. Mesh adaptation and discrete maximum principle for 2D anisotropic diffusion problems. Technical Report LA-UR 10-01227, Los Alamos National Laboratory, Los Alamos, NM, 2007.

[39] K. Lipnikov, M. Shashkov, D. Svyatskiy, and Y. Vassilevski. Monotone finite volume schemes for diffusion equations on unstructured triangular and shape-regular polygonal meshes. *J. Comput. Phys.*, 227:492–512, 2007.

[40] R. Liska and M. Shashkov. Enforcing the discrete maximum principle for linear finite element solutions of second-order elliptic problems. *Comm. Comput. Phys.*, 3:852–877, 2008.

[41] C. Lu, W. Huang, and J. Qiu. Maximum principle in linear finite element approximations of anisotropic diffusion-convection-reaction problems. *Numer. Math.* in press, 2012 (arXiv:1201.3564v1).

[42] M. J. Mlacnik and L. J. Durlofsky. Unstructured grid optimization for improved monotonicity of discrete solutions of elliptic equations with highly anisotropic coefficients. *J. Comput. Phys.*, 216:337–361, 2006.

[43] K. W. Morton and D. F. Mayers. *Numerical Solution of Partial Differential Equations*. Cambridge University Press, Cambridge, U.K., 2005. 2nd Edition.

[44] R. D. Russell, J. F. Williams, and X. Xu. MOVCOL4: a moving mesh code for fourth-order time-dependent partial differential equations. *SIAM J. Sci. Comput.*, 29:197–220 (electronic), 2007.

[45] P. Sharma and G. W. Hammett. Preserving monotonicity in anisotropic diffusion. *J. Comput. Phys.*, 227:123–142, 2007.

[46] G. Stoyan. On maximum principles for monotone matrices. *Lin. Alg. Appl.*, 78:147–161, 1986.

[47] G. Strang and G. J. Fix. *An Analysis of the Finite Element Method.* Prentice Hall, Englewood Cliffs, NJ, 1973.

[48] P. Sun, R. D. Russell, and J. Xu. A new adaptive local mesh refinement algorithm and its application on fourth order thin film flow problem. *J. Comput. Phys.*, 224:1021–1048, 2007.

[49] R. Temam. Une méthode d'approximation de la solution des équations de Navier-Stokes. *Bull. Soc. Math. France*, 96:115–152, 1968.

[50] V. Thomée and L. B. Wahlbin. On the existence of maximum principles in parabolic finite element equations. *Math. Comput.*, 77:11–19, 2008.

[51] J. Wang and R. Zhang. Maximum principle for P1-conforming finite element approximations of quasi-linear second order elliptic equations. *SIAM J Numer. Anal.*, 50:626–642, 2012. (arXiv:1105.1466).

[52] J. Xu and L. Zikatanov. A monotone finite element scheme for convection-diffusion equations. *Math. Comput.*, 69:1429–1446, 1999.

[53] X. Zhang and C.-W. Shu. On maximum-principle-satisfying high order schemes for scalar conservation laws. *J. Comput. Phys.*, 229:3091–3120, 2010.

[54] L. Zhornitskaya and A. L. Bertozzi. Positivity-preserving numerical schemes for lubrication-type equations. *SIAM J. Numer. Anal.*, 37:523–555, 2000.